# 0945060134 – 1

## Source Identification, Counterparts and Properties

### STONKS alert

This source is the same as: 0945060133 – 5.

- Type of Alert: First Detection,
- Long-term Variability $= 11.9$ for 0945060134 – 1 and $11.4$ for 0945060133 – 5,
- No short-term Variability.

Is the long-term variability negligeable between these two observations?

The long-term variability is the difference between the upper limit of the flux lowest value and the lower limit of the flux highest value.

The short-term variability is the result of a $\chi^2$ test of the flux against a constant value.

In the remainder of this document and for reasons of clarity and simplicity, we will refer to source 0945060134 – 1 as 34-1 and to source 0945060133 – 5 as 33-5.

### XMM-Newton Science Archive

https://nxsa.esac.esa.int/nxsa-web/#search

### Simbad

The source is not identified on Simbad.

### ESASky

On ESASky the pointer is on a green source, far from the nearest EPIC stack source. However, when looking at the image on XMM-Newton Science Archive, it would appear that it is indeed this green source (https://sky.esa.int/esasky/?target=53.59466666666666%20-28.902777777777782&hips=DSS2+color&fov=1&projection=SIN&cooframe=J2000&sci=true&lang=fr)

The source has multiple counterparts on ESASky:

- EPIC Stack (Soft X-ray),
- XMM-SUSS 6.2 (UV to Optical)? Slightly off,
- Gaia DR3 (Optical),
- Euclid MER Q1 (Optical to Near-IR),
- 2MASS (Near-IR),
- AllWISE (Near-IR to Mid-IR).

Gaia DR3 gives the following useful data:

- Parallax: $P = 2.941\ mas \rightarrow d \approx 340\ pc$,
- Magnitude: $G = 19.6951$,
- $G_{BP} - G_{RP} = 2.416$.

The source is faint and most likely Galactic.

Gaia DR3 also gives a probability of classification:

- Classprob Dsc Combmod Galaxy $= 9.9688 * 10^{-13}$,
- Classprob Dsc Combmod Quasar $= 9.0908 * 10^{-13}$,
- Classprob Dsc Combmod Star $= 1$.

The source is classified as a **star**.

There is no publication.

### 3DNH-tool

http://astro.uni-tuebingen.de/nh3d/nhtool

*3DNH-tool* suggests a column density of $n_H \approx 3 * 10^{20}\ cm^{-2}$, which is relatively low, typical of a Galactic source. However, this value might not be reliable as it does not account for the distance of the source.

## X-ray Periodicity

### Source 34-1

**PN:** Search with $f_0 \approx 0.0002\ s^{-1} \rightarrow P \approx 5000\ s$ and with $f_0 \approx 0.0001\ s^{-1} \rightarrow 5800\ s$.

**MOS2:** Search with $f_0 \approx 4.8\ s^{-1} \rightarrow P \approx 0.2\ s$, with $f_0 \approx 3.1\ s^{-1} \rightarrow P \approx 0.3\ s$ and with $f_0 \approx 1.2\ s^{-1} \rightarrow P \approx 0.8\ s$.

As the results differ between instruments, we chose to consider only those from the instrument with the highest maximum likelihood. According to the STONKS alert document, the maximum likelihood for PN is $DetML = 514.4$, while for M2 it is $DetML = 132.2$, supporting our decision to rely solely on the PN data.

### Source 33-5

The source exhibits no periodicity originally but because it is the same source as 34-1, we did a search with the frequency $f_0$ found for this last.

**PN:** Search with $f_0 \approx 0.0001\ s^{-1} \rightarrow P \approx 10000\ s$. Same for **MOS1** and **MOS2**.

The search with $f_0 \approx 0.0002\ s^{-1}$ gave no results.

#### Discussion

The periodicity of $5000\ s$ ($\sim 1.39\ h$) is consistent with a cataclysmic variable. Their orbital periods usually range from $4800\ s$ to $36000\ s$ ($\sim 80\ min$ to $\sim 10\ h$); There is even a known "period gap" between $7200\ s$ and $10800\ s$ ($\sim 2{-}\ 3\ h$) but systems still exist within and around this range.

A $5000\ s$ periodicity falls well within the CV orbital period regime, particularly on the shorter end, which is common for:

- Non-magnetic CVs (e.g., dwarf novae in quiescence)
- AM CVn systems (ultracompact helium-transferring binaries)

In magnetic CVs (e.g., intermediate polars), the white dwarf's spin period can often be detected as a strong X-ray periodicity.

- Typical spin periods range from a few hundred to several thousand seconds.
- A $5000\ s$ modulation could also represent the spin period in such a system.

# X-ray Spectral Properties

## Xspec models

The main models that we are using are: Black body, Bremsstrahlung, Apec, Powerlaw and Gauss, or a combination of two components: Black body and Powerlaw, Bremsstrahlung and Powerlaw, Gauss and Powerlaw, and, Apec and Apec.

### Black body

When an X-ray spectrum is well fitted by a black body model, it suggests that the X-ray emission is coming from a hot, dense surface or region that radiates like an ideal thermal emitter (i.e. a black body). A black body emits radiation with a spectrum that depends only on its temperature, and this emission is:

- Smooth and has a characteristic peak at a certain energy,
- Thermal, meaning it reflects a state of thermal equilibrium,
- Strongly dependent on temperature (the hotter the black body, the more it emits and the higher the peak energy).

A black body model fit generally implies that the X-rays are emitted by a compact and hot surface (not by diffuse gas). Likely sources include:

- The surface of a neutron star,
- The boundary layer in a white dwarf system (e.g., in cataclysmic variables),
- The accretion disk's inner region (if dense and hot enough),
- Or even a hot stellar photosphere.

### Bremsstrahlung

When a bremsstrahlung model (also known as thermal bremsstrahlung or free-free emission) fits an X-ray spectrum well, it suggests that the X-ray emission is primarily produced by hot, ionized gas (i.e. plasma) through a specific process: Bremsstrahlung (German for "braking radiation") occurs when electrons are decelerated as they pass near atomic nuclei. This deceleration causes them to lose energy in the form of X-ray photons. This type of emission is thermal, meaning the spectrum depends on the temperature of the plasma. A good fit with this model indicates that:

- The X-ray source likely contains hot plasma (temperatures typically in the range of millions of Kelvins, so $\sim 10^{-2} keV$ to $\sim keV$).
- The X-ray spectrum is smooth and continuous, without strong emission lines (although lines may still be present if other processes are involved).

It is common in environments like:

- Accretion shocks (e.g., in cataclysmic variables, where infalling material heats up).
- Stellar coronae (like in active M-dwarfs).
- Supernova remnants or galaxy clusters.

Source of the plasma temperature: https://www.sciencedirect.com/topics/earth-and-planetary-sciences/plasma-temperature.

## Astrophysical Plasma Emission Code (APEC)

When an X-ray spectrum is well fitted by an Apec model, it indicates that the emission is coming from a hot, diffuse, optically thin plasma in collisional ionization equilibrium. It models emission from a plasma that contains a mix of elements (H, He, Fe, etc.) at a certain temperature, where:

- Electrons collide with ions, exciting them,
- The ions then de-excite by emitting photons, often in the X-ray range,
- Both continuum emission (mainly bremsstrahlung) and emission lines are included in the model.

Thus, when Apec fits the spectrum, it suggests that:

- We are observing a thermal plasma (like bremsstrahlung, but with line emissions),
- The plasma is optically thin (photons escape without being absorbed),
- The plasma is in collisional ionization equilibrium, meaning the ionization state is stable and set by the temperature.

It is common in environments like:

- Stellar coronae (like in active M-dwarfs),
- Supernova remnants,
- Hot gas in galaxy clusters,
- Accretion disks or shocks in systems like cataclysmic variables (CVs),
- Flares, where gas is suddenly heated and emits thermal X-rays.

## Powerlaw

When an X-ray spectrum is well fit by a powerlaw model, it means that the emission is of non-thermal origin, meaning that it doesn't come from a hot gas or a thermal surface like in blackbody or bremsstrahlung models. Instead, it points to processes involving high-energy particles, such as acceleration or scattering. Mathematically, a powerlaw has the form:

$$F(E) \propto E^{-\Gamma} \tag{1}$$

With $F(E)$ the flux of photon at energy $E$ and $\Gamma$ the photon index (PhoIndex in *Xspec*) typically between 1 and 3. A steeper index (higher $\Gamma$) means the spectrum drops off faster with energy.

A good powerlaw fit implies non-thermal emission mechanisms, such as:

- Synchrotron radiation (relativistic electrons spiralling in magnetic fields),
- Inverse Compton scattering (high-energy electrons boosting low-energy photons),
- Emission from accretion flows, like in black holes or neutron stars,
- Emission from magnetically active stars (e.g. in the tail of a flare event).

We might see a powerlaw spectrum from:

- Active Galactic Nuclei (AGN) because of the non-thermal emission from jets or corona,
- X-ray binaries because of the accretion-powered emission with comptonization,
- Pulsars or magnetars because of the synchrotron and curvature radiation,
- Some flare stars or M-dwarfs because of high-energy particles in flare tails,
- Cataclysmic variables (CVs) if there is a strong magnetic activity or shock jets.

### Gauss

When an X-ray spectrum is well fit by a Gauss model, it means that one or more features in the spectrum, usually emission or absorption lines, are well described by a Gaussian function which is defined as:

$$f(E) = Ae^{-\frac{(E-E_0)^2}{2\sigma^2}} \tag{2}$$

Where $E$ is the energy (in $keV$ or $eV$), $E_0$ is the centroid energy (where the peak is), $\sigma$ is the standard deviation, related to the line width and $A$ is the amplitude, related to the line intensity.

A Gaussian profiles model spectral lines caused by atomic transitions if they are symmetric and not strongly broadened by complex physics (e.g., relativistic effects). So, if the spectrum is well fit by a Gauss model:

- There is likely a distinct emission or absorption line in the data,
- The line is symmetric and has a shape consistent with a Gaussian, suggesting relatively simple broadening mechanisms (e.g., thermal or instrumental),
- The Gaussian parameters can give physical information, such as:
    - Line center, which identifies the emitting/absorbing element or transition,
    - Line width, which gives insight into velocity dispersion, turbulence, or temperature,
    - Amplitude, which relates to the number of photons, hence the strength of the line.

Line centroid ($E_0$) can tell the ionization state of the emitting element. For example:

- $\sim 6.4\ keV$ → neutral $Fe$ (fluorescent line from reflection),
- $\sim 6.7\ keV$ → He-like Fe ($Fe\ 55$),
- $\sim 6.97\ keV$ → H-like Fe ($Fe\ 56$ ).

Line width ($\sigma$) can reveal turbulence, bulk motion, or instrumental broadening. A very broad line might hint at high-velocity material or blending of multiple unresolved lines.

Line amplitude combined with the continuum, gives info on abundances, emission measure, or plasma conditions.

In CVs for example, a $Fe\ K\alpha$ line at around $\sim 6.4\ keV$ might be modeled with a Gaussian as well as lines from other elements like O, Ne, Mg, Si. These lines are typically superimposed on the thermal continuum.

Seeing a Gaussian line in a CV spectrum might help confirm its identity. The Fe line complex is often used to distinguish magnetic CVs, especially intermediate polars, from other types of X-ray sources. Sometimes, a spectrum is fit with a thermal + one or more Gaussians to cleanly characterize both the continuum and the lines.

## Fit statistic

### Chi-squared

The chi-squared fit statistic assumes that each bin contains enough events to approximate the Poisson distribution with a normal distribution. If some bins have under 20 counts, this test becomes unreliable. In order to be more secure, we will consider that if the bins have less than 100 counts, C-statistic should be used instead. Here, we have about 95 counts which under 100 but still close, so we will do both Chi-squared and C-statistic.

The Chi-squared $\chi^2$ is the sum of the squared residuals, weighted by the errors in the data. The reduce Chi-squared $\chi_\nu^2$ (reduced by the number of degrees of freedom) is:

$$\chi_\nu^2 = \frac{\chi^2}{n_{bins} - n_{parameter}} \quad (2)$$

- $\chi_\nu^2 \approx 1$: Good fit.
- $\chi_\nu^2 \gg 1$: Bad fit.
- $\chi_\nu^2 \ll 1$: Overfitting?

Here, the number of bins is: $n_{bins} = 18$. The number of parameters $n_{parameter}$ depends on the model:

| Model | $n_{parameter}$ | Main parameters |
|---|---|---|
| tbabs*bbody | 3 | nH, kT, norm |
| tbabs*bremss | 3 | nH, kT, norm |
| tbabs*apec | 4 | nH, kT, abondance, norm |
| tbabs*powerlaw | 3 | nH, PhoIndex, norm |
| tbabs*(bbody+powerlaw) | 5 | nH, kT, norm (bbody), PhoIndex, norm (powerlaw) |
| tbabs*(bremss+powerlaw) | 5 | nH, kT, norm (bremss), PhoIndex, norm (powerlaw) |
| tbabs*(gauss+powerlaw) | 6 | nH, LineE, Sigma, norm (gauss), PhoIndex, norm (pow) |
| tbabs*(apec+apec) | 6 | nH, temp1, abondance, norm1, temp2, norm2 |

Let's compare the most promising models (i.e. with the chi-squared closest to 1):

| Criteria | Bremsstrahlung | Powerlaw | Bremsstrahlung + Powerlaw | Gauss + Powerlaw |
|---|---|---|---|---|
| Chi-squared $\chi^2$ | 14.5160 | 15.0731 | 12.4011 | 12.6865 |
| Reduce Chi-squared $\chi_\nu^2$ (5 bins) | 0.968 | 1.005 | 0.954 | 1.057 |
| Column density $n_H$ $(10^{22}\ cm^{-2})$ | 4.669e-02 ± 2.631e-02 | 0.142 ± 5.123e-02 | 5.813e-02 ± 3.204e-02 | 0.150 ± 5.333e-02 |
| $k_T$ $(keV)$ | 1.617 ± 0.42 | X | 1.380 ± 0.435 | X |
| PhoIndex $\Gamma$ | X | 2.600 ± 0.316 | -2.500 ± 3.616 | 2.659 ± 0.329 |
| Energy centroid $LineE$ $(keV)$ | X | X | X | 6.7 |
| Line width $\sigma$ | X | X | X | 4.756e-09 ±-1.00 |
| Norm | 2.007e-05 ± 4.406e-06 | 1.69e-05 ± 3.38e-06 | 2.259e-05 ± 6.481e-06 (bremss), 2.959e-09 ± 2.048e-08 (powerlaw) | 1.374e-06 ± 8.892e-07 (gauss), 1.742e-05 ± 3.579e-06 (powerlaw) |
| Null hypothesis probability | 4.868e-01 | 4.462e-01 | 4.951e-01 | 4.723e-01 |
| Degrees of freedom | 15 | 15 | 13 | 13 |

The Powerlaw model has a $X_\nu^2 = 1.005$ which is extremely close to 1, meaning it is almost a perfect fit. The Bremsstrahlung and Bremsstrahlung + Powerlaw models are also very good fit.

The column density value given by the Bremsstrahlung and Bremsstrahlung + Powerlaw models are the closest one to what 3DNH-tool suggest with $n_H \approx 5 * 10^{20}\ cm^{-2}$. The value of the column density of the Powerlaw and Gauss + Powerlaw models is: $n_H \approx 10^{21}\ cm^{-2}$, indicating a slightly farer source but still coherent. All imply a Galactic source.

The Bremsstrahlung and Bremsstrahlung + Powerlaw models have a temperature $k_T \approx\ 1.6\ keV$ and $k_T \approx\ 1.4\ keV$ respectively, which is consistent with hot plasmas, indicating possible coronal activity or accretion.

The Powerlaw and Gauss + Powerlaw models model yield a photon index $\Gamma \approx 2.6$, which is rather soft, and therefore more typical of certain non-thermal sources or a spectrum dominated by the diffuse background (synchrotron, inverse Compton), whereas the Bremsstrahlung + Powerlaw model gives a photon index of $\Gamma \approx -2.5$ with quite high uncertainties, which is not a satisfying result.

The Gauss + Powerlaw model fits best for the energy centroid set to $LineE = 6.7\ keV$ which correspond to $Fe\ 55$. The line width $\sigma$ is low but the uncertainty is very high. What can we say about it? Gauss model alone does not fit well at all.

The probabilities of the null hypothesis are equivalent $(\sim 0.46 - 0.5)$, so neither is statistically better although the Powerlaw model has a slightly lower probability.

### Discussion

The bremsstrahlung model suggests a thermal emitter like a **coronally active star** or **CV**; the powerlaw model with soft $\Gamma\ \approx\ 2.6$ could point to a **quiescent accreting system** like a **CV** or **X-ray binary**.

Based solely on the statistical quality of the fit, the Powerlaw model is slightly better.

## X-ray Flux and X-ray-to-Optical Flux Ratio

### Optical flux

The source is detected by Gaia DR3 with a magnitude $G\ =\ 19.6951$, a faint object which is consistent with a low-mass star at $340\ pc$.

The G-band corresponds to the wavelength interval of: 330 nm to 1050 nm (https://gaia.obspm.fr/la-mission/les-resultats/article/les-observations-spectro-photometriques).

The optical flux is calculated as follow:

$$\boldsymbol{F_{optical} = F_0 * 10^{-0.4*G}} \tag{3}$$

With $F_0 = 1.05 * 10^{-5}$ Gaia zero-point magnitude.

Here, we have an optical flux of $\boldsymbol{F_{optical} \approx 1.39 * 10^{-13}\ erg/cm^2/s}$.

### Typical X-ray flux to optical flux ratio

The typical X-ray flux to optical flux ratio of different sources is summaries in the following table:

| Object type | Typical $L_X$ range $(erg/s)$ |
|---|---|

| | |
|---|---|
| Active stars | $< 0.1$ |
| Cataclysmic variables | $\sim 0.1 - 10$ |
| AGNs | $> 1$ |

### X-ray flux to optical flux ratio of our source

#### Chi-squared

From *Xspec* AllModels.calcFlux(".2 12.0") we obtain the X-ray flux:

- Powerlaw model: $F_X \approx 4.66 * 10^{-14}\ erg/cm^2/s$,
- Bremsstrahlung model: $F_X \approx 4.06 * 10^{-14}\ erg/cm^2/s$,

So, an X-ray flux of $\boldsymbol{F_X \approx 4 * 10^{-14}\ erg/cm^2/s}$ regardless of the model.

Then, we calculate the X-ray to optical flux ratio:

- Powerlaw model: $\frac{F_X}{F_{optical}} \approx 0.34$.
- Bremsstrahlung model: $\frac{F_X}{F_{optical}} \approx 0.29$.

So, an X-ray to optical flux ratio of $\boldsymbol{\frac{F_X}{F_{optical}} \approx 0.3}$ regardless of the model.

### Discussion

This value doesn't contradict a **CV** interpretation:

- It supports a faint X-ray, optically visible Galactic object,
- It weakens the AGN hypothesis, which would typically show higher X-ray to optical dominance,
- It might slightly disfavor a highly magnetic CV, but a non-magnetic or mildly magnetic CV is still very plausible.

## Luminosity

### Typical luminosity

The typical luminosity of different sources is summaries in the following table:

| Object type | Typical $L_X$ range $(erg/s)$ |
|---|---|
| Active stars | $\sim 10^{28} - 10^{30}$ |
| Cataclysmic variables | $\sim 10^{30} - 10^{33}$ |
| Quiescent X-ray Binaries | $\sim 10^{31} - 10^{33}$ |
| AGNs | $> 10^{42}$ |

### Luminosity of our source

In order to calculate the luminosity $L$ in $erg/s$, the source is assumed to be spherical:

$$\boldsymbol{L = 4\pi F_X d^2} \qquad (4)$$

With $F_X$ the X-ray flux calculated previously in $erg/cm^2/s$ and $d$ the distance to the source in $cm$. This distance is calculated from value of the parallax given by Gaia: $P = 2.941\ mas$. We get a distance of $\boldsymbol{d \approx 1.05 * 10^{21}\ cm}$.

### Chi-squared

The luminosity of the source is:

- Powerlaw model: $L_X \approx 6.44 * 10^{29}\ erg/s$,
- Bremsstrahlung model: $L_X \approx 5.63 * 10^{29}\ erg/s$.

So, a luminosity of $\boldsymbol{L_X \approx 6 * 10^{29}\ erg/s}$ regardless of the model.

### Discussion

This luminosity is at the very low end (or even below) of CVs typical luminosity. It is more consistent with active stars.

## Documentations and Catalogues

### Antonio C. Rodriguez paper

https://doi.org/10.1088/1538-3873/ad357c

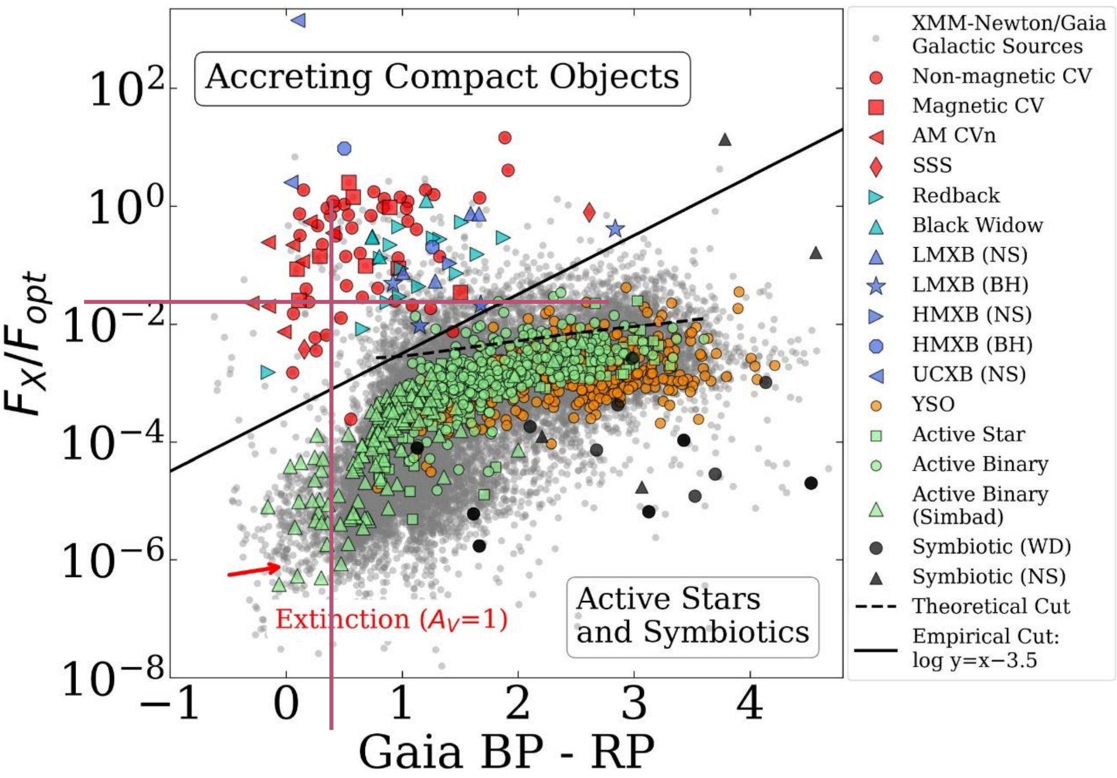


*Figure 1. X-ray Main Sequence. Galactic sources from the XMM-Newton/Gaia crossmatch are shown in grey. Accreting compact object binaries in the upper left are separated from symbiotic and active stars on the bottom right by the "empirical cut" (solid line) or "theoretical cut" (dotted line). All classifications on the right-side panel are from the literature, and described in Section 2.3. No extinction correction is applied here, but the extinction vector is shown (de-reddening slides sources toward the lower left).*

Gaia gives: $G_{BP} - G_{RP} = 2.416$ and we previously calculated the ratio: $\frac{F_X}{F_{optical}} \approx 0.3$. Reporting these values on the figure (pink lines) our source points above the theorical and empirical cuts indicating an accreting compact object binary, particularly in the area of non-magnetic CV, magnetic CV and AM CVn.

## Tommaso Maccacaro et al. paper

https://articles.adsabs.harvard.edu/pdf/1988ApJ...326..680M

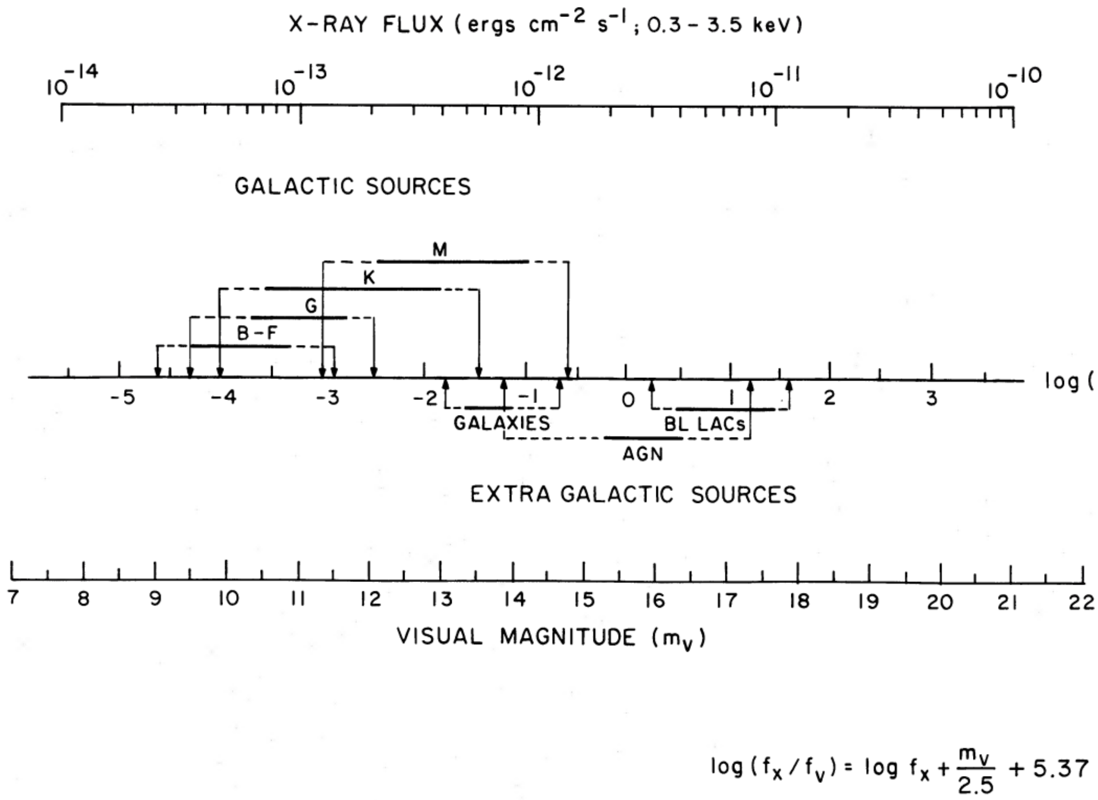


*Figure 1. Nomograph to compute the log[fx/fv], given the X-ray flux and the visual magnitude of a source. The correspondance between the various classes of X-ray sources and their typical log[fx/fv] is also indicated.*

The figure presents a nomograph to compute the $\log\left(\frac{f_X}{f_v}\right)$ given the X-ray flux $f_X$ in the $0.3-3.5\ keV$ band in ergs/cm^2/s and the visual magnitude $m_v$ of the source:

$$\log\left(\frac{f_X}{f_v}\right) = \log(f_X) + \frac{m_v}{2.5} + 5.37 \tag{5}$$

With $f_v$ the visual flux.

For $m_v$ we take the magnitude $G = 19.6951$ given by Gaia DR3, as previously.

### Chi-squared

From *Xspec* AllModels.calcFlux(".3 3.5") we obtain the X-ray flux:

- Powerlaw model: $f_X \approx 3.54 * 10^{-14}\ erg/cm^2/s$.
- Bremsstrahlung model: $f_X \approx 3.59 * 10^{-14}\ erg/cm^2/s$.

The logarithm is then:

- Powerlaw model: $\log\left(f_X/\mathrm{f_v}\right) \approx -0.202$.
- Bremsstrahlung model: $\log\left(f_X/\mathrm{f_v}\right) \approx -0.196$.

So, a logarithm of $\mathbf{\log\left(f_X/f_v\right) \approx -0.2}$ which corresponds to AGN.

Where are CVs on this figure?

The Maccacaro result is ambiguous because it classifies AGN based on high X-ray-to-optical ratio; but does not exclude CVs, which can have overlapping values. Moreover, AGNs are extragalactic and far more luminous than the low luminosity we found, contradicting the AGN interpretation.

The Rodriguez diagram is more recent and tuned for Galactic sources. Since the source is likely Galactic, the Rodriguez figure has more weight.

### Dacheng Lin, Natalie Webb et al. paper

https://dx.doi.org/10.1088/0004-637X/756/1/27

The Dacheng Lin, Natalie Webb et al. paper discusses multi-wavelength data using X-ray hardness ratio.

### XMM-Athena Catalogue

https://xmm-ssc.irap.omp.eu/xmm2athena/catalogues/

Unclassified.

## Possible Classifications

### Cataclysmic variables

CVs are binary systems where a white dwarf accretes matter from a companion star. In magnetic CVs (polars, intermediate polars), the accretion flow can produce strong shock-heated plasma, leading to hard X-ray emission.

CV is a strong candidate due to:

Source Identification, Counterparts and Properties

- Galactic counterpart with stellar classification,
- Multiwavelength detection: EPIC Stack (Soft X-ray), XMM-SUSS 6.2 (UV to Optical), Gaia DR3 (Optical), Euclid MER Q1 (Optical to Near-IR), 2MASS (Near-IR) and AllWISE (Near-IR to Mid-IR),
- Distance from parallax $P = 2.941\ mas \to d \approx 340\ pc$, so it is most likely Galactic,
- Gaia DR3 classification as a star.

X-ray Variability and Periodicity

- Period of $5000\ s$.

X-ray Spectral Properties

- Spectral fits consistent with thermal emission (Bremsstrahlung) and soft power law, Gauss + Power-law?
- Soft power law index: $\Gamma \approx 2.5 - 2.6$ and thermal emission: $k_T \approx 1.4 - 1.6\ keV$ ,
- Moderate absorption: $n_H \approx 10^{20} - 10^{21}\ cm^{-2}$,
- X-ray flux: $F_X \approx 4 * 10^{-14}\ erg/cm^2/s$,
- X-ray to optical flux ratio: $\frac{F_X}{F_{optical}} \approx 0.3$, supporting non-magnetic or mildly magnetic CV,
- Antonio C. Rodriguez paper figure 1: accreting compact object binary, particularly in the area of non-magnetic CV, magnetic CV and AM CVn.

However, the luminosity $L_X \approx 10^{29}\ erg/s$ is very low for a CV, even in quiescence.

## Active Star

Active star is a strong candidate due to:

Source Identification, Counterparts and Properties

- Galactic counterpart with stellar classification,
- Multiwavelength detection: EPIC Stack (Soft X-ray), XMM-SUSS 6.2 (UV to Optical), Gaia DR3 (Optical), Euclid MER Q1 (Optical to Near-IR), 2MASS (Near-IR) and AllWISE (Near-IR to Mid-IR),
- Faint: $G = 19.6951$,
- Distance from parallax $P = 2.941\ mas \rightarrow d \approx 340\ pc$, so it is most likely Galactic,
- Gaia DR3 classification as a star.

X-ray Variability and Periodicity

- Period of $5000\ s$, could match stellar rotation or binary orbit.

X-ray Spectral Properties

- Spectral fits consistent with thermal emission (Bremsstrahlung) and soft power law,
- Soft power law index: $\Gamma \approx 2.5 - 2.6$ and thermal emission: $k_T \approx 1.4 - 1.6\ keV$, fit with coronal emission of active stars,
- Moderate absorption: $n_H \approx 10^{20} - 10^{21}\ cm^{-2}$,
- X-ray flux: $F_X \approx 4 * 10^{-14}\ erg/cm^2/s$,
- Luminosity $L_X \approx 10^{29}\ erg/s$ matches active stars.

However, the X-ray to optical flux ratio: $\frac{F_X}{F_{optical}} \approx 0.3$ is high for active stars and Antonio C. Rodriguez paper figure 1 shows that the source is more an accreting compact object binary, particularly in the area of non-magnetic CV, magnetic CV and AM CVn.

# Conclusion

The evidence supports that source **34-1/33-5** could be a:

- coronally active star, such as a late-type dwarf (e.g. M-dwarf), showing long-term variability and moderate X-ray emission, possibly with a rotational period of ~5000 s.
- galactic CV, most likely a non-magnetic with a $5000\ s$ orbital period.

AGN hypothesis is unsupported given the Gaia parallax and X-ray luminosity.

# References

## Astronomical databases

XMM-Newton Science Archive (https://nxsa.esac.esa.int/nxsa-web/#search).

ESASky (https://sky.esa.int/esasky/?target=53.59466666666666%20-28.902777777777782&hips=DSS2+color&fov=1&projection=SIN&cooframe=J2000&sci=true&lang=fr).

3DNHTOOL (http://astro.uni-tuebingen.de/nh3d/nhtool).

XMM-Athena catalogue (https://xmm-ssc.irap.omp.eu/xmm2athena/catalogues/).

## Journal

ScienceDirect (https://www.sciencedirect.com/topics/earth-and-planetary-sciences/plasma-temperature).

## Scientific papers

Kado-Fong, E. et al. (2016), *M Dwarf Activity in the Pan-STARRS1 Medium-Deep Survey: First Catalog and Rotation Periods*, The Astrophysical Journal, Volume 833, Issue 2, article id. 281, 19 pp. (https://ui.adsabs.harvard.edu/abs/2016ApJ...833..281K/abstract).

Antonio C. Rodriguez (2024), *From Active Stars to Black Holes: A Discovery Tool for Galactic X-Ray Sources*, PASP **136** 054201 (https://doi.org/10.1088/1538-3873/ad357c).

Tommaso Maccacaro et al. (1988), *The X-ray spectra of the extragalactic sources in the einstein extended medium sensitivity survey*, The Astrophysical Journal, 326:680-690 (https://articles.adsabs.harvard.edu/pdf/1988ApJ...326..680M).

Dacheng Lin et al. (2012), *Classification of x-ray sources in the XMM-Newton serendipitous source catalog*, ApJ **756** 27 (https://dx.doi.org/10.1088/0004-637X/756/1/27

L. Mignon et al. (2023), *Characterisation of stellar activity of M dwarfs. I. Long-timescale variability in a large sample and detection of new cycles*, A&A 675, A168 (https://doi.org/10.1051/0004-6361/202244249).

Emily K. Pass et al. (2023), *Active Stars in the Spectroscopic Survey of Mid-to-late M Dwarfs within 15 pc*, The Astronomical Journal, 166:16 (14pp) (https://iopscience.iop.org/article/10.3847/1538-3881/acd6a2).

## Website

https://gaia.obspm.fr/la-mission/les-resultats/article/les-observations-spectro-photometriques